arXiv:1609.04590v2 [hep-ph] 12 Oct 2016

Higgs boson couplings in multi-doublet models with natural flavour conservation

Kei Yagyu[1]

[1]*School of Physics and Astronomy, University of Southampton, Southampton, SO17 1BJ, United Kingdom**

We investigate the deviation in the couplings of the standard model (SM) like Higgs boson (h) with a mass of 125 GeV from the prediction of the SM in multi-doublet models within the framework where flavour changing neutral currents at the tree level are naturally forbidden. After we present the general expressions for the modified gauge and Yukawa couplings for h, we show the correlation between the deviation in the Yukawa coupling for the tau lepton $h\tau^+\tau^-$ and that for the bottom quark $hb\bar{b}$ under the assumption of a non-zero deviation in the hVV ($V = W, Z$) couplings in two Higgs doublet models (2HDMs) and three Higgs doublet models (3HDMs) as simple examples. We clarify the possible allowed prediction of the deviations in the 3HDMs which cannot be explained in the 2HDMs even taking into account the one-loop electroweak corrections to the Yukawa coupling.

I. INTRODUCTION

The observation of the discovered Higgs boson $h(125)$ with decaying into a pair of tau leptons [1, 2] provided more evidence for the existence of at least one $SU(2)_L$ doublet scalar field in addition to various other measurements of the properties of $h(125)$ at the CERN Large Hadron Collider (LHC). Then, the natural question is "how many doublet fields are there in the Higgs sector?" In general, multi-Higgs doublet models (MHDMs) can reproduce the predictions of the standard model (SM) composed of only one Higgs doublet, and so we should take into account the possibility of the existence of multi-doublets.

On the other hand, multi-doublet fields arise in many models beyond the SM. As the most familiar example, in the minimal supersymmetric SM (MSSM) the Higgs sector is extended

*Electronic address: K.Yagyu@soton.ac.uk

to have two doublets because of the requirement of gauge anomaly cancellation. In addition, the multi-doublet structure is required to have an additional source of CP-violation, which is necessary to realize the successful scenario of electroweak baryogenesis [3–5]. Moreover, additional doublets are often introduced in various loop-induced neutrino mass models, such as the model by Zee [6] and by Ma [7] etc. The point is that the structure of MHDMs depends on new physics scenarios, e.g., in the MSSM the so-called Type-II Yukawa interaction is adopted. Therefore, by studying the phenomenology of MHDMs with a bottom-up approach, we can narrow down the possible scenarios of new physics beyond the SM.

One of the most important issues when MHDMs are discussed is the possibility of flavour changing neutral currents (FCNCs) mediated by neutral Higgs bosons, which appear at the tree level in general. The simplest way to avoid such FCNCs is to realize a Yukawa Lagrangian where each type of fermion, i.e., charged leptons, up-type and down-type quarks couples to only one scalar doublet field. This is usually achieved by imposing discrete symmetries in the Higgs sector, and is so-called "natural flavour conservation" (NFC) [8]. Depending on how doublet fields couple to each type of fermions, there are four (five) independent types of Yukawa interactions in models with two (more than two) doublets [9].

In this paper, we discuss the deviation in the couplings of $h(125)$ to weak bosons (hVV and $V = W, Z$) and fermions ($hf\bar{f}$) from the SM prediction in the MHDMs with NFC. In Ref. [10], it has been clarified that the four types of Yukawa interactions in two Higgs doublet models (2HDMs) can be determined by measuring the correlation between the deviations in the charged lepton Yukawa couplings $he\bar{e}$ and the down-type quark Yukawa couplings $hd\bar{d}$ as long as there is a non-zero deviation in the hVV couplings. Now, we extend this discussion to models with N Higgs doublet fields, and we investigate how the pattern of the deviation can be different in 2HDMs and in MHDMs with $N \geq 3$.

This paper is organized as follow. In Sec. II, we define the MHDMs with NFC. We then give the general expressions for the hVV and $hf\bar{f}$ couplings. We show more explicit forms of these couplings in the 2HDMs and the three Higgs doublet models (3HDMs) as simple examples. In Sec. III, we give numerical results of the deviation in the couplings of $h(125)$ especially for the $h\tau^+\tau^-$ and $hb\bar{b}$ couplings in the 2HDMs and the 3HDMs. Conclusions are given in Sec. IV.

II. MULTI-DOUBLET MODELS

A. Higgs Basis

We consider models with N Higgs doublet fields[1] Φ_i $(i = 1, \ldots, N)$ with hypercharge[2] $Y = +1/2$ and vacuum expectation values (VEVs) $v_i \equiv \sqrt{2}\langle \Phi_i^0 \rangle$ which are taken to be real. Throughout this paper, we assume that the Higgs sector has neither explicit nor spontaneous CP-violation for simplicity. In order to extract couplings among physical Higgs bosons and gauge bosons or fermions, it is convenient to define the so-called Higgs basis [11], where only one of the N doublets has the VEV v which is related to the Fermi constant G_F by $v = (\sqrt{2}G_F)^{-1/2} \simeq 246$ GeV. The Higgs basis is defined via the $N \times N$ orthogonal matrix R by

$$\begin{pmatrix} \Phi_1 \\ \Phi_2 \\ \vdots \\ \Phi_N \end{pmatrix} = R \begin{pmatrix} \Phi \\ \Psi_2 \\ \vdots \\ \Psi_N \end{pmatrix}. \tag{1}$$

The doublets Φ and Ψ_a $(a = 2, \ldots, N)$ appearing in the right-hand side of Eq. (1) are expressed as

$$\Phi = \begin{pmatrix} G^+ \\ \frac{\tilde{H}+v+iG^0}{\sqrt{2}} \end{pmatrix}, \quad \Psi_a = \begin{pmatrix} \tilde{H}_a^+ \\ \frac{\tilde{H}_a+i\tilde{A}_a}{\sqrt{2}} \end{pmatrix}, \tag{2}$$

where $G^\pm$ and G^0 are the Nambu-Goldstone bosons which are absorbed into the longitudinal components of the $W^\pm$ and Z bosons, respectively. In Eq. (1), the matrix R is expressed in terms of $N-1$ angles, so that the N VEVs are translated into v and the $N-1$ angles. By using R, each of VEVs is expressed as

$$v_i = R_{i1} v, \tag{3}$$

and the sum rule: $\sum_i v_i^2 = v^2 \sum_i R_{i1}^2 = v^2$ follows from this equation. In the Higgs basis, the $N-1$ pairs of singly-charged states $\tilde{H}_a^\pm$, $N-1$ CP-odd states $\tilde{A}_a$ and N CP-even states

[1] The number of doublets can be constrained from the electroweak oblique S and T parameters. In Ref. [12], the maximally allowed number of doublets has been given as a function of a mass difference among Higgs bosons.

[2] The electric charge Q is given by $Q = T_3 + Y$ with T_3 being the third component of the isospin.

$\tilde{H}_i \equiv (\tilde{H}, \tilde{H}_a)$ are not mass eigenstates in general. Their mass eigenstates can be defined by introducing $(N-1)\times(N-1)$ unitarity matrices $R_\pm$ and R_A for the singly-charged states and CP-odd states and an $N \times N$ unitary matrix R_H for the CP-even states as

$$\tilde{H}^\pm_a = (R_\pm)_{ab} H^\pm_b, \quad \tilde{A}_a = (R_A)_{ab} A_b, \quad \tilde{H}_i = (R_H)_{ij} H_j. \tag{4}$$

We identify the $h \equiv H_1$ state as the discovered Higgs boson with a mass of 125 GeV.

Let us move on to the construction of the kinetic term and the Yukawa Lagrangian for the scalar doublets in the Higgs basis. Without loss of generality, the kinetic term is expressed as follows:

$$\mathcal{L}_{\rm kin} = |D_\mu \Phi|^2 + \sum_{a=2}^{N} |D_\mu \Psi_a|^2, \tag{5}$$

where D_μ is the covariant derivative for the doublet Higgs fields. From the above Lagrangian, the gauge-gauge-scalar type interaction is obtained from the first term, because only Φ contains the VEV v. Thus, we can extract the couplings of h with weak bosons as

$$g_{hVV} = (R_H)_{11} \times g^{\rm SM}_{hVV}, \quad V = W,\ Z, \tag{6}$$

where we take $0 \le (R_H)_{11} \le 1$. We note that from the second term in Eq. (5), we obtain the scalar-scalar-gauge type interactions which are proportional to the derivative of a scalar field. These interaction terms can be important when we consider production and decay of extra Higgs bosons.

Next, we give the Yukawa Lagrangian. In the scenario based on NFC, the Yukawa Lagrangian takes the following form:

$$-\mathcal{L}_Y = \bar{Q}_L\, Y_u\, \tilde{\Phi}_u u_R + \bar{Q}_L\, Y_d\, \Phi_d d_R + \bar{L}_L\, Y_e\, \Phi_e e_R + \text{h.c.}, \tag{7}$$

where $\Phi_{u,d,e}$ are any one of Φ_i, and $\tilde{\Phi} = i\sigma_2 \Phi^*$ with σ_2 being the second Pauli matrix. Here, we do not explicitly show the flavour indices. The Lagrangian given in Eq. (7) is naturally realized by imposing discrete symmetries such as Z_N for models with N Higgs doublet fields. Under such a discrete symmetry, all the N doublets can have a distinct charge from each other. Depending on the charge assignment for the right-handed fermions[3], there appear

[3] The charge assignment for the right-handed fermions should be taken as the flavour blind way to obtain the Lagrangian given in Eq. (7).

five independent types of Yukawa interactions. They can be defined as follows:

$$\text{Type-I} : \Phi_u = \Phi_d = \Phi_e, \tag{8a}$$

$$\text{Type-II} : \Phi_u \neq \Phi_d, \quad \Phi_d = \Phi_e, \tag{8b}$$

$$\text{Type-X} : \Phi_u = \Phi_d, \quad \Phi_d \neq \Phi_e, \tag{8c}$$

$$\text{Type-Y} : \Phi_u \neq \Phi_d, \quad \Phi_u = \Phi_e, \tag{8d}$$

$$\text{Type-Z} : \Phi_u \neq \Phi_d, \quad \Phi_d \neq \Phi_e, \quad \Phi_e \neq \Phi_u. \tag{8e}$$

A similar classification of the Yukawa interactions has been presented in Ref. [13]. We note that the Type-II, Type-X and Type-Y (Type-Z) are realized for $N \geq 2$ ($N \geq 3$).

The Yukawa Lagrangian can be rewritten in the Higgs basis as

$$\begin{aligned} -\mathcal{L}_Y =& \frac{\sqrt{2}}{v}\left[\bar{Q}_L M_u \left(\tilde{\Phi} + \sum_{a=2}^{N} \xi_u^a \tilde{\Psi}_a\right) u_R + \bar{Q}_L M_d \left(\Phi + \sum_{a=2}^{N} \xi_d^a \Psi_a\right) d_R \right. \\ & \left. + \bar{L}_L M_e \left(\Phi + \sum_{a=2}^{N} \xi_e^a \Psi_a\right) e_R\right] + \text{h.c.}, \end{aligned} \tag{9}$$

where M_u, M_d and M_e are respectively the mass matrix for up-type quarks, down-type quarks and charged leptons, which are given by $M_F = v Y_F R_{F1}/\sqrt{2}$ for $F = u, d, e$. The ξ_F^a factors are determined by the matrix elements of R as follows:

$$\xi_F^a = \frac{R_{Fa}}{R_{F1}}, \quad a = 2, \ldots, N. \tag{10}$$

In terms of $(R_H)_{ij}$ and ξ_F^a, the Yukawa couplings for h are expressed by

$$y_{hFF} = \left[(R_H)_{11} + \sum_{a=2}^{N} (R_H)_{a1} \xi_F^a\right] \times y_{hFF}^{\rm SM}. \tag{11}$$

In order to express the deviations in the Higgs boson couplings, we introduce the scaling factor for the gauge couplings by $\kappa_V \equiv g_{hVV}/g_{hVV}^{\rm SM}$ and for the Yukawa couplings by $\kappa_F \equiv y_{hFF}/y_{hFF}^{\rm SM}$. We can express κ_F using $\kappa_V = (R_H)_{11}$ by

$$\kappa_F = \kappa_V + \sum_{a=2}^{N} (R_H)_{a1} \xi_F^a, \quad \text{with} \quad \sum_{a=2}^{N} (R_H)_{a1}^2 = 1 - \kappa_V^2. \tag{12}$$

From the above expression, it is seen that κ_F become unity by taking the limit of $\kappa_V \to 1$, and this limit is the so-called "alignment limit" [14]. We thus can regard h as the SM-like Higgs boson for the case with $\kappa_V \simeq 1$. Because of the existence of the alignment limit, the

	2HDM			3HDM					
	ξ_u	ξ_d	ξ_e	ξ_u^2	ξ_d^2	ξ_e^2	ξ_u^3	ξ_d^3	ξ_e^3
Type-I	$\cot\beta$	$\cot\beta$	$\cot\beta$	$\cot\beta_1$	$\cot\beta_1$	$\cot\beta_1$	0	0	0
Type-II	$\cot\beta$	$-\tan\beta$	$-\tan\beta$	$\cot\beta_1$	$-\tan\beta_1$	$-\tan\beta_1$	0	$-\tan\beta_2/\cos\beta_1$	$-\tan\beta_2/\cos\beta_1$
Type-X	$\cot\beta$	$\cot\beta$	$-\tan\beta$	$\cot\beta_1$	$\cot\beta_1$	$-\tan\beta_1$	0	0	$-\tan\beta_2/\cos\beta_1$
Type-Y	$\cot\beta$	$-\tan\beta$	$\cot\beta$	$\cot\beta_1$	$-\tan\beta_1$	$\cot\beta_1$	0	$-\tan\beta_2/\cos\beta_1$	0
Type-Z	–	–	–	$\cot\beta_1$	$-\tan\beta_1$	$-\tan\beta_1$	0	$-\tan\beta_2/\cos\beta_1$	$\cot\beta_2/\cos\beta_1$

TABLE I: ξ_F^a factors appearing in Eq. (11) for each type of Yukawa interaction in the 2HDM and the 3HDM. In the 2HDM, the ξ_F^2 factors are rewritten by ξ_F.

MHDMs can safely reproduce predictions in the SM. Notice here that in MHDMs, κ_V must be smaller or equal to unity at the tree level[4]. On the other hand, $|\kappa_F|$ can be both smaller and larger than unity due to the second term of Eq. (12).

B. Examples

Based on the general discussion given in the previous subsection, we here consider two simple examples, i.e., the case for $N = 2$ (2HDMs) and for $N = 3$ (3HDMs).

In the 2HDMs[5], the matrix R takes the 2×2 form as

$$R = \begin{pmatrix} c_\beta & -s_\beta \\ s_\beta & c_\beta \end{pmatrix}, \quad \text{for} \quad N = 2, \tag{13}$$

where $\tan\beta \equiv v_2/v_1$. We introduce shorthand notations for the trigonometric functions as c_θ (s_θ) $= \cos\theta$ ($\sin\theta$). From Eqs. (10) and (13), we can find that ξ_F^2 (notice that the superscript 2 does not mean the square of ξ_F) is taken to be either $\cot\beta$ or $-\tan\beta$ depending on the type of Yukawa interaction and the type of fermion. If we fix $\Phi_u = \Phi_2$, all the $\xi_F \equiv \xi_F^2$ factors are fixed for each type of Yukawa interaction and for each type of fermion as shown in Table I. In addition, the matrix R_H also takes 2×2 form with an angle[6] independent of

[4] If we introduce higher $SU(2)_L$ multiplets such as triplets, $\kappa_V > 1$ is possible at the tree level [15].
[5] For a comprehensive review on 2HDMs, see Ref. [16].
[6] This angle depends on parameters in the scalar potential. In this paper, we do not explicitly show the

β. Conventionally, this angle is expressed by $\beta - \alpha$ (see e.g., [17]), so that R_H is written as

$$R_H = \begin{pmatrix} s_{\beta-\alpha} & c_{\beta-\alpha} \\ c_{\beta-\alpha} & -s_{\beta-\alpha} \end{pmatrix}. \tag{14}$$

Because of the orthogonal property of the R_H matrix, $(R_H)_{21} (= c_{\beta-\alpha})$ appearing in Eq. (12) is simply written by $\sigma\sqrt{1-\kappa_V^2}$ with $\sigma = \mathrm{Sign}[(R_H)_{21}]$, and thus κ_F is determined by $\tan\beta$, κ_V and σ. Then, κ_F can be rewritten by

$$\Delta\kappa_F = -\Delta\kappa_V + \sigma\,\xi_F\sqrt{(2-\Delta\kappa_V)\Delta\kappa_V} \simeq -\Delta\kappa_V + \sigma\,\xi_F\sqrt{2\Delta\kappa_V}, \tag{15}$$

where $\Delta\kappa_V \equiv 1 - \kappa_V$ (≥ 0) and $\Delta\kappa_F \equiv \kappa_F - 1$. The far-right hand side is valid for $\kappa_V \simeq 1$ which is supported by the current measurement at the LHC [18]. We note that because of the $\sigma\,\xi_F$ term of Eq. 15, we can take the so-called "wrong sign limit" [19] defined by $\Delta\kappa_F \to -2$. The case with this limit or this regime provides a phenomenologically interesting scenario, where loop induced decay rates such as $h \to gg$ and $h \to \gamma\gamma$ can be modified from the SM prediction due to effects of interference even having the same or similar value of the decay rate of $h \to VV$ and $h \to f\bar{f}$ as those in the SM at the tree level.

Eq. (15) tells us the following important fact. As long as $|\xi_F| > \sqrt{\Delta\kappa_V/(2-\Delta\kappa_V)}\,(\leq 1)$, the sign of $\Delta\kappa_F$ is determined by the sign of $\sigma\,\xi_F$. In this case, the prediction of $(\Delta\kappa_e, \Delta\kappa_d)$ in the four types of Yukawa interactions appears in the four different quadrant on the $\Delta\kappa_e$–$\Delta\kappa_d$ plane for a fixed σ which can be determined by measuring the sign of $\Delta\kappa_u$. Namely for $\Delta\kappa_u > 0$, the sign of $(\Delta\kappa_e, \Delta\kappa_d)$ is predicted by $(+,+)$, $(-,-)$, $(-,+)$ and $(+,-)$ in the Type-I, -II, -X and -Y Yukawa interaction, respectively, while for $\Delta\kappa_u < 0$ these signs are flipped as compared to the former case. Therefore, by the precise measurements of $\Delta\kappa_e$ and $\Delta\kappa_d$, we can determine the type of Yukawa interaction in the 2HDM.

Although this statement is valid for the case with $|\xi_F| > \sqrt{\Delta\kappa_V/(2-\Delta\kappa_V)}$ for all F as mentioned above, the case with at least one of $|\xi_F|$ being smaller than $\sqrt{\Delta\kappa_V/(2-\Delta\kappa_V)}$ is phenomenologically quite difficult to realize in the Type-II, -X and -Y 2HDM, which is explained following. In order to achieve[7] $\xi_u (= \cot\beta) < \sqrt{\Delta\kappa_V/(2-\Delta\kappa_V)}$, we need a rather

potential whose structure depends not only on the number of doublets but also on the symmetry to avoid the tree level FCNCs.

[7] For $\xi_F = -\tan\beta$, the condition $|\xi_F| > \sqrt{\Delta\kappa_V/(2-\Delta\kappa_V)}$ is satisfied unless we take $\tan\beta < 1$ which is disfavored by the various B physics constraints mainly due to the enhancement of the top Yukawa coupling. See, e.g., [20, 21] for the constraints on the parameter space from B physics in 2HDMs.

large value of $\tan\beta$ if $\Delta\kappa_V \ll 1$. For example, when $\Delta\kappa_V$ is given to be 5% (1%), $\tan\beta$ should be larger than about 6 (14) to satisfy $\cot\beta < \sqrt{\Delta\kappa_V/(2-\Delta\kappa_V)}$. The important point is that such a case gives a huge deviation in some of Yukawa couplings in the Type-II, -X, and -Y 2HDM. In fact in the Type-II 2HDM, $\Delta\kappa_e (= \Delta\kappa_d) \simeq 180\%\,(200\%)$ for the case of $\Delta\kappa_V = 5\%\,(1\%)$, $\tan\beta = 6\,(14)$ and $\sigma = -1$. Similarly in the Type-X (Type-Y) 2HDM, $\Delta\kappa_e$ ($\Delta\kappa_d$) becomes the above value, and it goes without saying that such a huge deviation has already been excluded by the current data at the LHC [18]. Therefore, if $|\xi_F| < \sqrt{\Delta\kappa_V/(2-\Delta\kappa_V)}$ is realized, only the Type-I 2HDM provides a phenomenologically acceptable scenario.

Next, we consider the 3HDMs. In this case, the matrix R takes the 3×3 form, and its one of the explicit forms is given by [22]

$$R = \begin{pmatrix} c_{\beta_2} & 0 & -s_{\beta_2} \\ 0 & 1 & 0 \\ s_{\beta_2} & 0 & c_{\beta_2} \end{pmatrix} \begin{pmatrix} c_{\beta_1} & -s_{\beta_1} & 0 \\ s_{\beta_1} & c_{\beta_1} & 0 \\ 0 & 0 & 1 \end{pmatrix} = \begin{pmatrix} c_{\beta_1}c_{\beta_2} & -s_{\beta_1}c_{\beta_2} & -s_{\beta_2} \\ s_{\beta_1} & c_{\beta_1} & 0 \\ c_{\beta_1}s_{\beta_2} & -s_{\beta_1}s_{\beta_2} & c_{\beta_2} \end{pmatrix}, \quad \text{for} \quad N=3, \tag{16}$$

where $\tan\beta_1 \equiv v_2/\sqrt{v_1^2+v_3^2}$ and $\tan\beta_2 \equiv v_3/v_1$. A similar but different parameterization of the three VEVs has also been given in Ref. [23]. Using this notation, each of ξ_F^a factors are expressed as in Table I, where we assign $\Phi_u = \Phi_2$, and $\Phi_{d,e} = \Phi_1$ (if these are different from Φ_u) in the Type-II, -X and -Y interactions. For the Type-Z, we assign $(\Phi_u, \Phi_d, \Phi_e) = (\Phi_2, \Phi_1, \Phi_3)$. Unlike the 2HDMs, the second term of Eq. (12) is not simply determined by κ_V, so that to get the prediction of κ_F, we need to further input $(R_H)_{21}$ and $(R_H)_{31}$ under the constraint of $(R_H)_{21}^2 + (R_H)_{31}^2 = 1-\kappa_V^2$.

We here discuss critical differences of the Higgs boson couplings between in the 2HDMs and in the 3HDMs. First, as it is immediately seen, the Type-Z Yukawa interaction is only realized in 3HDMs. In other words in 2HDMs, there is at least one pair of κ_F and $\kappa_{F'}$ ($F \neq F'$) with $\kappa_F = \kappa_{F'}$ as seen in (8), while the Type-Z can provide the prediction of $\kappa_u \neq \kappa_d$, $\kappa_d \neq \kappa_e$ and $\kappa_e \neq \kappa_u$. Next, in 2HDMs the prediction of $\Delta\kappa_d \neq \Delta\kappa_e$ with $\Delta\kappa_{d,e} > 0$ or $\Delta\kappa_{d,e} < 0$ is not allowed as explained by the following. First of all, $\Delta\kappa_d \neq \Delta\kappa_e$ is realized in the Type-X and Type-Y 2HDM. However, in these types, e.g., in the Type-X, $\xi_e = -\tan\beta$ and $\xi_d = \cot\beta$. Therefore for a fixed σ, the sign of $\Delta\kappa_e$ is opposite to that of $\Delta\kappa_d$ as long as $|\xi_F| > \sqrt{\Delta\kappa_V/(2-\Delta\kappa_V)}$. On the other hand, this is not the case for the 3HDMs as it will numerically be shown in the next section.

III. DEVIATION IN THE HIGGS BOSON COUPLINGS

In this section, we show the correlation between $\Delta\kappa_\tau$ and $\Delta\kappa_b$ in the 2HDMs and in the 3HDMs. We choose the following parameters as inputs:

$$\Delta\kappa_V,\ \tan\beta,\ \sigma,\ \text{ for the 2HDMs,} \tag{17}$$

$$\Delta\kappa_V,\ \tan\beta_1,\ \tan\beta_2,\ (R_H)_{21},\ \sigma',\ \text{ for the 3HDMs,} \tag{18}$$

where $\sigma' \equiv \mathrm{Sign}[(R_H)_{31}]$. In these input parameters for the 3HDM, $|(R_H)_{31}|$ is derived by $\sqrt{1-\kappa_V^2-[(R_H)_{21}]^2}$. For all the calculations below, we scan the value of $(R_H)_{21}$ in the range from $-\sqrt{1-\kappa_V^2}$ to $+\sqrt{1-\kappa_V^2}$. In order to clarify the possible allowed predictions in the 3HDMs which cannot be explained in the 2HDMs, we take into account the one-loop electroweak corrections to the Yukawa couplings in the 2HDMs based on the on-shell renormalization scheme[8] according to Refs. [24, 25]. For the one-loop calculation, we scan the parameters of the 2HDM by $m_\Phi \geq 300$ GeV, $\tan\beta \geq 1$ and $|\lambda_{h\Phi\Phi}| \geq 0$ with $\lambda_{h\Phi\Phi} \equiv (m_\Phi^2 - M^2)/v$, where m_Φ is the mass of extra Higgs bosons (here we assume that all the extra Higgs bosons are degenerate in mass), and M [26] is a dimensionful parameter which is irrelevant to the Higgs VEV (see, e.g., [24] for the detailed explanation about these parameters). For the SM inputs, we use the following values [27]

$$\begin{aligned}
&m_t = 173.21\ \text{GeV},\ m_b = 4.66\ \text{GeV},\ m_c = 1.275\ \text{GeV},\ m_\tau = 1.77684\ \text{GeV},\ m_h = 125\ \text{GeV},\\
&\alpha_{\rm em} = (137.035999074)^{-1},\ m_Z = 91.1876\ \text{GeV},\ G_F = 1.1663787\times 10^{-5}\ \text{GeV}^{-2},\\
&\Delta\alpha_{\rm em} = 0.06635,\ \alpha_s = 0.1185\ \text{GeV}.
\end{aligned} \tag{19}$$

We take into account theoretical constraints on the model parameters from the perturbative unitarity [28–31], the vacuum stability [32], and the triviality with the criterion that the Landau pole does not appear below 3 TeV. We note that the amount of QCD corrections to the $hb\bar{b}$ coupling can be a sub percent level in the SM [33], which are not included in our calculation.

First, we show the difference of the prediction of $\Delta\kappa_\tau$ and $\Delta\kappa_b$ in the 2HDMs with four types of Yukawa interaction. In Fig. 1, we show the correlation between $\Delta\kappa_\tau$ and $\Delta\kappa_b$ in

[8] In Ref. [34], improved renormalization schemes in the 2HDM have been proposed where gauge dependences in the mixing angles are successfully removed.

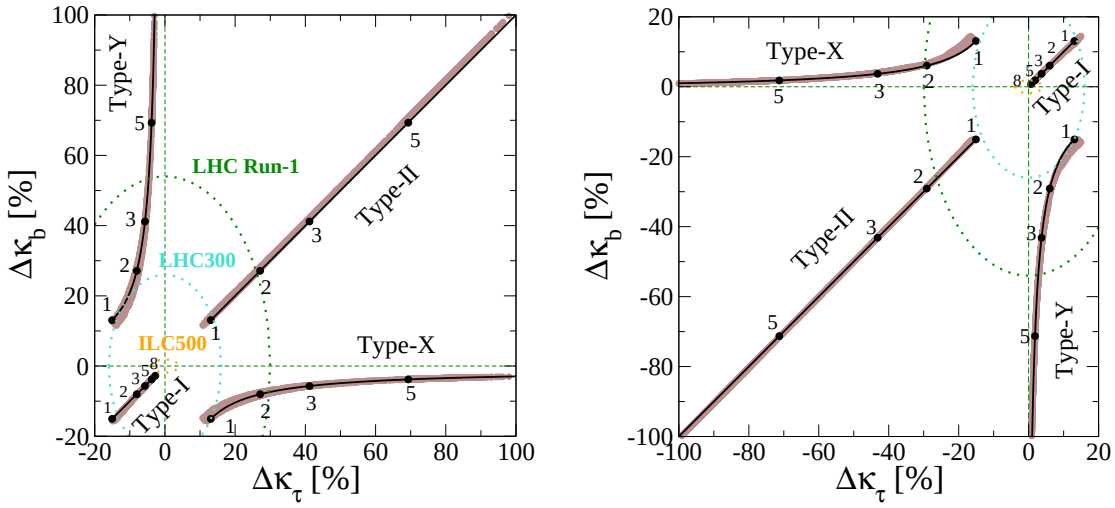

FIG. 1: Predicitons on the $\Delta\kappa_\tau$ and $\Delta\kappa_b$ plane in the Type-I, -II, -X and -Y 2HDMs in the case of $\Delta\kappa_V = 1\%$. The solid curves show the tree level prediction. Each dot on these curves denotes the prediction of the fixed value of $\tan\beta$, where its value is written beside the dot. The gray shaded regions show the one-loop corrected results. The left and right panels respectively show the case for $\sigma = -1$ and $\sigma = +1$. The largest (green) dotted ellipse shows the 2σ error of the measurement of $\Delta\kappa_\tau$ and $\Delta\kappa_b$ from the current LHC data extracted from Ref. [18], while the middle (cyan) and smallest (orange) ones respectively show the expected 2σ accuracy of the measurement at the LHC with the collision energy of 14 TeV and the integrated luminosity of 300 fb^{-1} and at the ILC with the collision energy of 500 GeV and the integrated luminosity of 500 fb^{-1}) extracted from [35].

the four types of Yukawa interaction in the 2HDM. We here take $\Delta\kappa_V (= 1 - (R_H)_{11}) = 1\%$, $\tan\beta \geq 1$ and $\sigma = -1$ $(+1)$ in the left (right) panel. The solid curves show the tree level prediction, while the shaded regions do the one-loop corrected result. We can see that the predictions of the four types of Yukawa interaction are well separated in the $\Delta\kappa_\tau$–$\Delta\kappa_b$ plane even taking into account the one-loop correction to the Yukawa couplings. In this figure, we display the 2σ error of the measurement of $\Delta\kappa_\tau$ and $\Delta\kappa_b$ at the LHC Run-1 experiment[9] by the green dotted ellipse, where data from the ATLAS and CMS collaborations are combined [18]. In addition, we also show the expected 2σ accuracy of the measurement of $\Delta\kappa_\tau$ and $\Delta\kappa_b$ at the LHC with 14 TeV and 300 fb^{-1} (denoted as

[9] Here, we extract the 2σ errors of Δ_τ and Δ_b from Ref. [18], but we do not use their central values.

LHC300) and at the International Linear Collider (ILC) with 500 GeV and 500 fb^{-1} (denoted as ILC500). Although the current measurement (LHC Run-1) is not enough accurate to separate the four types of Yukawa interaction in the configuration with $\Delta\kappa_V = 1\%$, we may be able to discriminate these types of Yukawa interaction by the future measurements at the LHC300 and the ILC500. We note that for a larger (smaller) value of $\Delta\kappa_V$, the distance of each prediction in the four types of Yukawa interaction becomes to be more (less) spread. As the extreme case, when $\Delta\kappa_V \to 0$ is taken, all the predictions converge at $(\Delta\kappa_\tau, \Delta\kappa_b) \to (0, 0)$.

Next, we compare the prediction of $\Delta\kappa_\tau$ and $\Delta\kappa_b$ in the 2HDM and in the 3HDM. Because in the Type-I and Type-II case, tree level predictions in both the 2HDM and the 3HDM are given on the line of $\Delta\kappa_b = \Delta\kappa_\tau$, it is difficult to see the difference between these two models. We thus compare the prediction in the Type-X and Type-Y Yukawa interaction. In Fig. 2, we show the correlation between $\Delta\kappa_\tau$ and $\Delta\kappa_b$ in the 2HDM and in the 3HDM in the case of $\Delta\kappa_V = 1\%$. The results for the Type-X (Type-Y) are given in the left (right) panel, while those in the case for $\Delta\kappa_u < 0$ ($\Delta\kappa_u > 0$) are displayed in the upper (lower) panel. Clearly, we can find the region which cannot be drawn by the one-loop corrected prediction in the 2HDM, but can be explained in the 3HDM. We note that in the 3HDMs with a larger (smaller) value of $\tan\beta_2$, each of the parabolas becomes that with a larger (small) curvature through the same point given in the 2HDM denoted by the black dot.

Finally, we show the prediction in the Type-Z 3HDM on the $\Delta\kappa_\tau$ and $\Delta\kappa_b$ plane. The left and right panel show the case for $\Delta\kappa_u < 0$ and $\Delta\kappa_u > 0$, respectively. We can see that the predictions with $\Delta\kappa_{\tau,b} > 0$ ($\Delta\kappa_{\tau,b} < 0$) and $\Delta\kappa_\tau \neq \Delta\kappa_b$ are allowed for the case of $\Delta\kappa_u < 0$ ($\Delta\kappa_u > 0$), which are not allowed in the 2HDMs at the tree level. Even if we take into account the one-loop corrections to the Yukawa coupling, only a few percent level of the difference between $\Delta\kappa_\tau$ and $\Delta\kappa_b$ is allowed as we see in Fig. 1. Therefore, if the Higgs boson couplings are measured to be in this region, i.e., $\Delta\kappa_{\tau,b} > 0$ ($\Delta\kappa_{\tau,b} < 0$) and $\Delta\kappa_\tau \neq \Delta\kappa_b$, it can be evidence for the MHDMs with $N \geq 3$.

IV. CONCLUSIONS

We have studied the SM-like Higgs boson couplings with weak bosons hVV and fermions $hf\bar{f}$ in MHDMs with NFC. We have presented the generic expression for the scaling factors

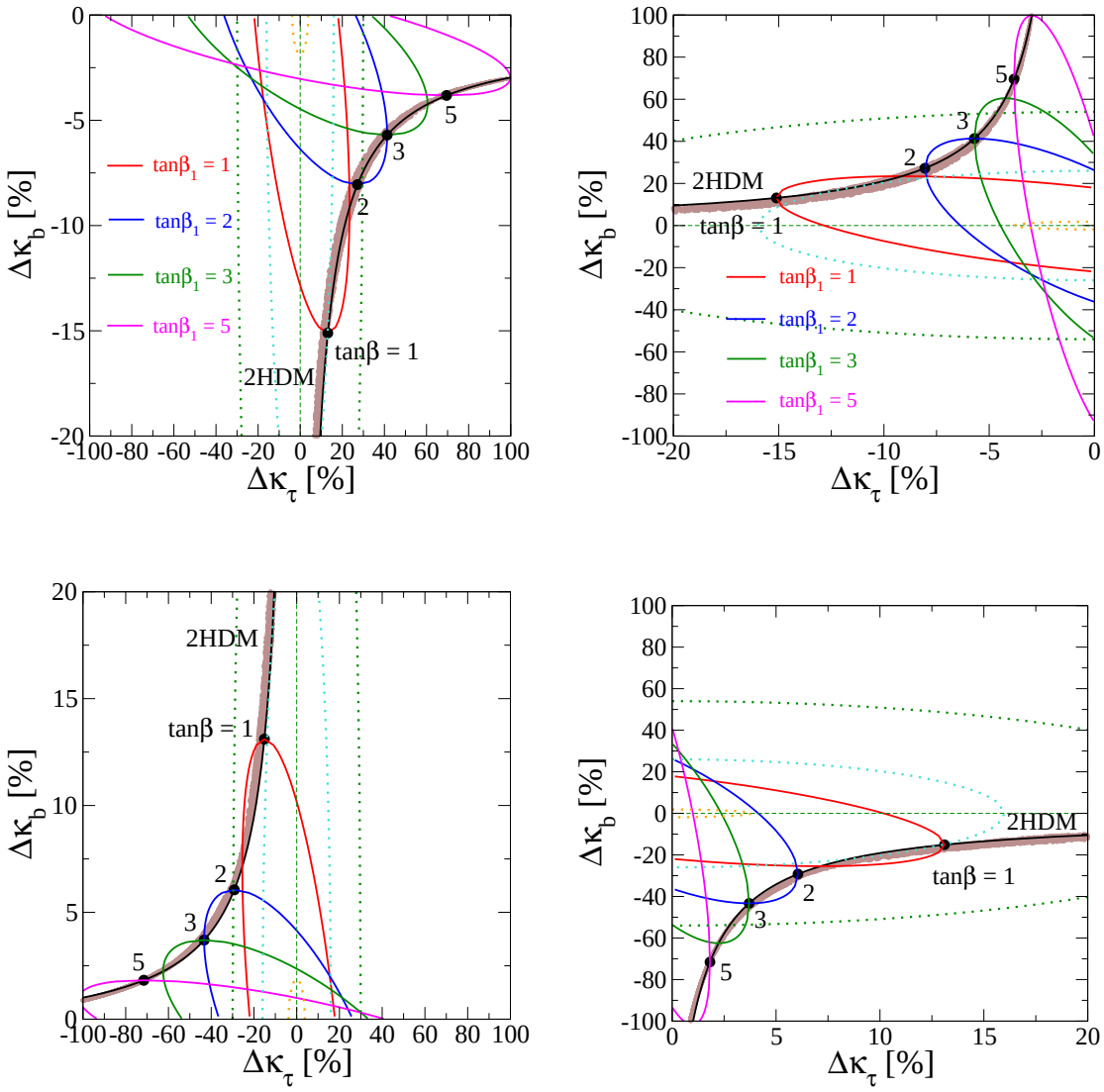

FIG. 2: Predicitons of $\Delta\kappa_\tau$ and $\Delta\kappa_b$ in the 2HDM and in the 3HDM in the case of $\Delta\kappa_V = 1\%$. The left-upper, right-upper, left-lower and right-lower panel respectively shows the case for (Type-X, $\Delta\kappa_u < 0$), (Type-Y, $\Delta\kappa_u < 0$), (Type-X, $\Delta\kappa_u > 0$) and (Type-Y, $\Delta\kappa_u > 0$). Similar to Fig. 1, the black curve shows the tree level prediction, and the gray shaded region does the one-loop corrected result in the 2HDM. The red, blue, green and magenta curve respectively shows the tree level prediction in the 3HDM with $\tan\beta_1 = 1$, 2, 3 and 5 in the 3HDM. For all the results in the 3HDM, we take $\tan\beta_2 = 1$. The description of the three ellipses is the same as those in Fig. 1.

of κ_V and κ_F in the model with N doublet scalar fields. As simple concrete examples, we have discussed the 2HDMs and the 3HDMs, and have presented the formulae of these scaling factors in terms of the ratios of the Higgs VEVs and the matrix elements of the

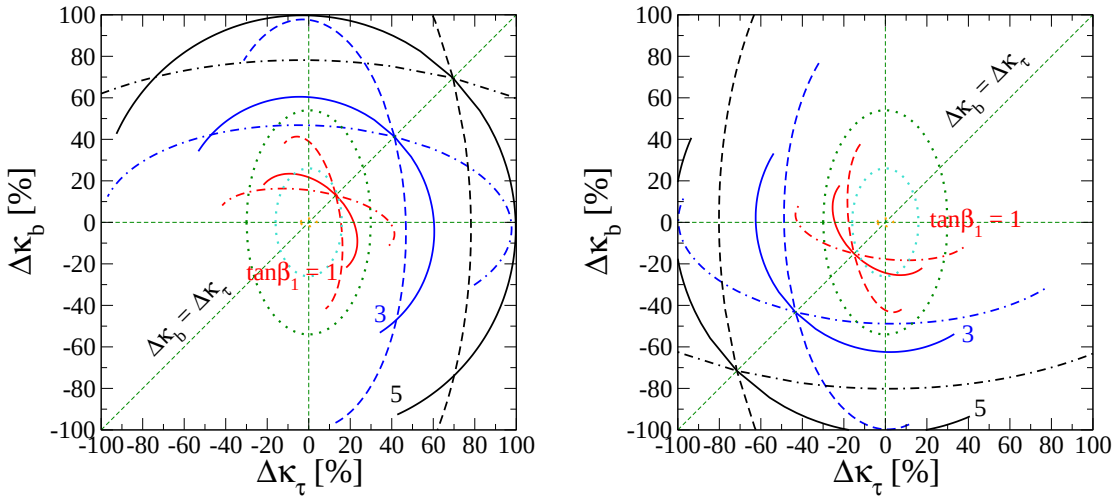

FIG. 3: Predicitons of $\Delta\kappa_\tau$ and $\Delta\kappa_b$ in the Type-Z 3HDM in the case of $\Delta\kappa_V = 1\%$. The left (right) panel shows the case for $\Delta\kappa_u < 0$ ($\Delta\kappa_u > 0$). The value of $\tan\beta_2$ is taken to be 1 (solid curve), 2 (dashed curve) and 1/2 (dotted curve). The description of the three ellipses is the same as that in Fig. 1.

diagonalization matrix for the CP-even scalar states for each type of Yukawa interaction. We then have shown the correlation between $\Delta\kappa_\tau$ and $\Delta\kappa_b$ in the 2HDMs and in the 3HDMs under the assumption that the hVV couplings deviate from the SM prediction by 1%. It has been clarified that there are predictions in the $\Delta\kappa_\tau$ and $\Delta\kappa_b$ plane in the 3HDMs, which cannot be explained in the 2HDMs even when taking into account the one-loop corrections to the Yukawa coupling.

We would like to mention that such a region can also be explained within a 2HDM if we relax the framework of NFC such as the so-called Type-III 2HDM. However, in such a model FCNCs mediated by neutral Higgs bosons are naturally induced, so that measurements at flavour experiments also become important to discriminate the models with NFC and those without NFC.

Finally, we briefly comment on the case with CP-violation in the Higgs sector which is assumed not being occurred in this paper. If there is a non-zero physical CP-violating phase in the Higgs potential, CP-even and CP-odd component scalar fields are mixed with each other. Through the mixing, the Yukawa coupling for the SM-like Higgs boson contains a term proportional to the γ_5 matrix, which can modify various physical quantities such as decay rates and cross sections of the SM-like Higgs boson from the SM prediction even if

$\kappa_F = 1$ is taken. The collider phenomenology with such a CP-violating effect has been studied in Refs. [36–38] in the 2HDMs. In addition, the method to extract the CP-even component (without γ_5) and the CP-odd component (with γ_5) of the $ht\bar{t}$ coupling has been proposed in Ref. [39] by measuring the $ht\bar{t}$ cross section weighted by an operator constructed from the (anti-)top quark momentum.

Acknowledgments

The author is grateful to Shinya Kanemura for fruitful discussions. He also thanks to Andrew Akeroyd for careful reading of the manuscript. This work was supported by a JSPS postdoctoral fellowships for research abroad.

[1] G. Aad *et al.* [ATLAS Collaboration], JHEP **1504**, 117 (2015) [arXiv:1501.04943 [hep-ex]].

[2] S. Chatrchyan *et al.* [CMS Collaboration], JHEP **1405**, 104 (2014) [arXiv:1401.5041 [hep-ex]].

[3] N. Turok and J. Zadrozny, Phys. Rev. Lett. **65**, 2331 (1990).

[4] A. I. Bochkarev, S. V. Kuzmin and M. E. Shaposhnikov, Phys. Rev. D **43**, 369 (1991).

[5] A. E. Nelson, D. B. Kaplan and A. G. Cohen, Nucl. Phys. B **373**, 453 (1992).

[6] A. Zee, Phys. Lett. B **93**, 389 (1980) [Erratum-ibid. B **95**, 461 (1980)].

[7] E. Ma, Phys. Rev. D **73**, 077301 (2006) [hep-ph/0601225].

[8] S. L. Glashow and S. Weinberg, Phys. Rev. D **15**, 1958 (1977).

[9] Y. Grossman, Nucl. Phys. B **426**, 355 (1994).

[10] S. Kanemura, K. Tsumura, K. Yagyu and H. Yokoya, Phys. Rev. D **90**, 075001 (2014) [arXiv:1406.3294 [hep-ph]].

[11] S. Davidson and H. E. Haber, Phys. Rev. D **72**, 035004 (2005) [Phys. Rev. D **72**, 099902 (2005)]. [hep-ph/0504050].

[12] A. E. Crcamo Hernndez, S. Kovalenko and I. Schmidt, Phys. Rev. D **91**, 095014 (2015) [arXiv:1503.03026 [hep-ph]].

[13] P. M. Ferreira, L. Lavoura and J. P. Silva, Phys. Lett. B **688**, 341 (2010) [arXiv:1001.2561 [hep-ph]].

[14] P. S. Bhupal Dev and A. Pilaftsis, JHEP **1412**, 024 (2014) Erratum: [JHEP **1511**, 147 (2015)] [arXiv:1408.3405 [hep-ph]].

[15] S. Kanemura, M. Kikuchi and K. Yagyu, Phys. Rev. D **88**, 015020 (2013) [arXiv:1301.7303 [hep-ph]].

[16] G. C. Branco, P. M. Ferreira, L. Lavoura, M. N. Rebelo, M. Sher and J. P. Silva, Phys. Rept. **516**, 1 (2012) [arXiv:1106.0034 [hep-ph]].

[17] J. F. Gunion, H. E. Haber, G. L. Kane and S. Dawson, Front. Phys. **80**, 1 (2000).

[18] G. Aad *et al.* [ATLAS and CMS Collaborations], JHEP **1608**, 045 (2016) [arXiv:1606.02266 [hep-ex]].

[19] P. M. Ferreira, J. F. Gunion, H. E. Haber and R. Santos, Phys. Rev. D **89**, no. 11, 115003 (2014) [arXiv:1403.4736 [hep-ph]].

[20] F. Mahmoudi and O. Stal, Phys. Rev. D **81**, 035016 (2010). [arXiv:0907.1791 [hep-ph]].

[21] T. Enomoto and R. Watanabe, JHEP **1605**, 002 (2016) [arXiv:1511.05066 [hep-ph]].

[22] A. G. Akeroyd, S. Moretti, K. Yagyu and E. Yildirim, arXiv:1605.05881 [hep-ph].

[23] J. L. Diaz-Cruz and U. Saldana-Salazar, arXiv:1405.0990 [hep-ph].

[24] S. Kanemura, M. Kikuchi and K. Yagyu, Phys. Lett. B **731**, 27 (2014) [arXiv:1401.0515 [hep-ph]].

[25] S. Kanemura, M. Kikuchi and K. Yagyu, Nucl. Phys. B **896**, 80 (2015) [arXiv:1502.07716 [hep-ph]].

[26] S. Kanemura, Y. Okada, E. Senaha and C.-P. Yuan, Phys. Rev. D **70**, 115002 (2004) [hep-ph/0408364].

[27] K. A. Olive *et al.* [Particle Data Group Collaboration], Chin. Phys. C **38**, 090001 (2014).

[28] S. Kanemura, T. Kubota and E. Takasugi, Phys. Lett. B **313**, 155 (1993).

[29] A. G. Akeroyd, A. Arhrib and E. M. Naimi, Phys. Lett. B **490**, 119 (2000). [arXiv:hep-ph/0006035].

[30] I. F. Ginzburg and I. P. Ivanov, Phys. Rev. D **72**, 115010 (2005).

[31] S. Kanemura and K. Yagyu, Phys. Lett. B **751**, 289 (2015) [arXiv:1509.06060 [hep-ph]].

[32] N. G. Deshpande and E. Ma, Phys. Rev. D **18**, 2574 (1978).

[33] G. P. Lepage, P. B. Mackenzie and M. E. Peskin, arXiv:1404.0319 [hep-ph].

[34] M. Krause, R. Lorenz, M. Muhlleitner, R. Santos and H. Ziesche, arXiv:1605.04853 [hep-ph].

[35] S. Dawson *et al.*, arXiv:1310.8361 [hep-ex].

[36] A. Barroso, P. M. Ferreira, R. Santos and J. P. Silva, Phys. Rev. D **86**, 015022 (2012) [arXiv:1205.4247 [hep-ph]].

[37] D. Fontes, J. C. Romo, R. Santos and J. P. Silva, Phys. Rev. D **92**, no. 5, 055014 (2015) [arXiv:1506.06755 [hep-ph]].

[38] V. Keus, S. F. King, S. Moretti and K. Yagyu, JHEP **1604**, 048 (2016) [arXiv:1510.04028 [hep-ph]].

[39] J. F. Gunion and X. G. He, Phys. Rev. Lett. **76**, 4468 (1996) [hep-ph/9602226].